

Photoinduced Dissociation and Desorption of N₂O on a Pt(111) SurfaceJ. Kiss,[†] D. Lennon, S. K. Jo, and J. M. White*

46

Department of Chemistry and Center for Materials Chemistry, The University of Texas at Austin, Austin, Texas 78712 (Received: January 14, 1991)

N₂O adsorbed on a Pt(111) surface was irradiated by UV light from a mercury arc lamp. The photochemistry of N₂O was studied by XPS, UPS, and TPD. Upon irradiation at 50 K, adsorbed N₂O undergoes dissociation and desorption. Photon energies exceeding 4.35 eV are required. The cross section is in the range of 10⁻¹⁹–10⁻²⁰ cm². The data are adequately described with a model involving subvacuum hot electrons.

1. Introduction

Despite the strong quenching of electronically excited states by substrate metal,^{1,2} it has now been well established that photon-driven adsorbate bond breaking and desorption occurs for many adsorbed molecules. Photochemical processes can compete with electronic quenching on metal substrates. Much effort is being focused on the elucidation of the underlying mechanism and the distinction between different excitation paths, e.g. direct valence electronic excitation and substrate-generated electron hole excitation.³⁻⁵ To extend the work in our laboratory, we have investigated the UV photochemistry of N₂O on Pt(111). This system was chosen as both the photochemistry⁶ and the electron-induced chemistry⁷⁻⁹ of N₂O in the gas phase are known and N₂O is used as an electron scavenger in radiolysis experiments.¹⁰

The surface science of N₂O has been examined on Pt(111)¹¹ as well as other metals. N₂O adsorbs molecularly on Pt(111)¹¹ and Ir(111).¹² It partly dissociates, leaving oxygen on the surface on W(110),¹³ Ni films,¹⁴ Ni(100),¹⁵ Ni(110),¹⁶ Al(100),¹⁷ Ag(111),¹⁸ and Ru(001).¹⁹⁻²¹ HREELS results indicate that N₂O adsorbs linearly, but tilted with respect to the surface normal, in the monolayer range on Pt(111), whereas the second N₂O layer lies approximately parallel to the surface.¹¹

To our knowledge, there has been no previous report of UV photon-driven chemistry in this system. We show here, by using temperature-programmed desorption (TPD), X-ray photoelectron spectroscopy (XPS), and ultraviolet photoelectron spectroscopy (UPS), that both desorption and dissociation of N₂O occur on Pt(111) irradiated with photons whose energies exceed 4.35 eV. The results are described in terms of a hot-electron attachment model.

2. Experimental Section

A standard UHV chamber, equipped with XPS, UPS, and TPD capabilities, was used. A closed-cycle He cryostat (APD Cryogenics) was applied to cool the crystal to 50 K. The ionizer of the quadrupole mass spectrometer was covered with a grounded Ta-foil shield that had a 15-mm-diameter sampling snout covered with stainless steel mesh. This ensured preferential detection of molecules desorbing from the crystal surface and minimized previously noted electron-stimulated desorption and dissociation effects.²¹ The hemispherical analyzer was operated at a pass energy of 40 eV for UPS and XPS. Binding energies are referenced to the Fermi level. A heating rate of 4.3 K/s was used to TPD. The sample temperature was monitored with a chromel-alumel thermocouple spot-welded to the back of the crystal. The sample was cleaned by Ne⁺ ion sputtering and oxidation treatments followed by high-temperature annealing. The cleanliness of the sample was checked by XPS.

N₂O (>99% purity) was used without further purification, and dosed into the Pt(111) surface through a 2- μ m pinhole. A linear motion driver was used to bring the end of the doser to within 2 mm of the crystal surface. This procedure minimizes adsorption

on, and desorption from, surfaces other than the Pt(111) front face and is helpful in TPD.

Adsorbate-covered surfaces were irradiated, through a UV-grade sapphire window, with a 100-W high-pressure Hg arc lamp (Photon Technology Inc.) A 10-mm aperture was used to restrict the light to the sample surface. With this setup, the maximum photon energy at the sample was not greater than 5.4 eV (the onset of UV intensity from the Hg arc lamp). The incident power flux delivered to the crystal at full arc was 100 mW/cm², measured outside the chamber with a power meter under otherwise the same optical and geometric conditions. The temperature rise of the crystal during irradiation did not exceed 8 K. The wavelength distribution was varied by the use of cutoff filters. The light was incident at 45° off the surface normal, and the axis of the hemispherical electron energy analyzer was located along the surface normal. With this geometry, we could measure the relative photoelectron signal during UV irradiation.

3. Results

3.1. Thermal Chemistry of N₂O on a Pt(111) Surface. 3.1.1. TDS Results. Adsorption of N₂O on clean Pt(111) at 50 K occurs molecularly, in agreement with earlier work.¹¹ Figure 1 shows a series of TPD spectra of N₂O at different exposures. Two distinct desorption peaks were obtained, one at 97–102 K and the other at 75–87 K (multilayer). One monolayer (ML) coverage was defined as the maximum exposure that gave no multilayer peak. At very low exposures a single desorption peak developed around 102 K. The peak position continuously shifted to lower temperatures with increasing coverage up to 0.3 ML and then remained constant, centered at 97 K. When the monolayer was almost saturated, a second peak appeared at around 75 K. This

- (1) Avouris, P.; Persson, B. N. J. *J. Phys. Chem.* **1984**, *88*, 837.
- (2) Chance, R. R.; Prock, A.; Silbey, R. *J. Chem. Phys.* **1975**, *62*, 2245.
- (3) Zhou, X.-L.; Zhu, X.-Y.; White, J. M. *Acc. Chem. Res.* **1990**, *23*, 327.
- (4) Ho, W. *Comments Condens. Matter Phys.* **1988**, *13*, 293.
- (5) Zhou, X.-L.; Zhu, X.-Y.; White, J. M. *Surf. Sci. Rep.*, submitted for publication.
- (6) Oakabe, H. *Photochemistry of Small Molecules*; Wiley: New York, 1978.
- (7) Christophoru, L. G. *Atomic and Molecular Radiation Physics*; Wiley-Interscience: New York, 1971.
- (8) Christophoru, L. G. *Electron-Molecule Interactions and Their Applications*; Academic Press: New York, 1984; Vols. 1 and 2.
- (9) Massey, H. *Negative Ions*; Cambridge University Press: Cambridge, U.K., 1976.
- (10) Baxendale, J. H.; Wardman, P. *The Radiolysis of Methanol*; NSRDS-NBS 54; U.S. National Bureau of Standards: Washington, DC, 1975.
- (11) Avery, N. R. *Surf. Sci.* **1983**, *235*, 501.
- (12) Cornish, J. C. L.; Avery, N. R. *Surf. Sci.* **1990**, *235*, 209.
- (13) Fuggle, J. C.; Menzel, D. *Surf. Sci.* **1979**, *79*, 1.
- (14) Brundle, C. R., *J. Vac. Sci. Technol.* **1976**, *13*, 301.
- (15) Hoffman, D. A.; Hudson, J. B. *Surf. Sci.* **1987**, *180*, 77.
- (16) Sau, R.; Hudson, J. B. *J. Vac. Sci. Technol.* **1981**, *18*, 607.
- (17) Pashutski, A.; Folman, M. *Surf. Sci.* **1989**, *216*, 395.
- (18) Grimblot, J.; Alnot, P.; Behm, R. J.; Brundle, C. R. *J. Electron Spectrosc. Relat. Phenom.* **1990**, *52*, 175.
- (19) Umbach, E.; Menzel, D. *Chem. Phys. Lett.* **1981**, *84*, 491.
- (20) Madey, T. E.; Avery, N. R.; Anton, A. B.; Toby, B. H.; Weinberg, W. H. *J. Vac. Sci. Technol.* **1983**, *1*, 1220.
- (21) Kim, Y.; Schreifels, J. A.; White, J. M. *Surf. Sci.* **1982**, *114*, 349.

[†] Permanent address: Reaction Kinetics Research Group of Hungarian Academy of Sciences, University of Szeged, P.O. Box 105, Szeged, Hungary.

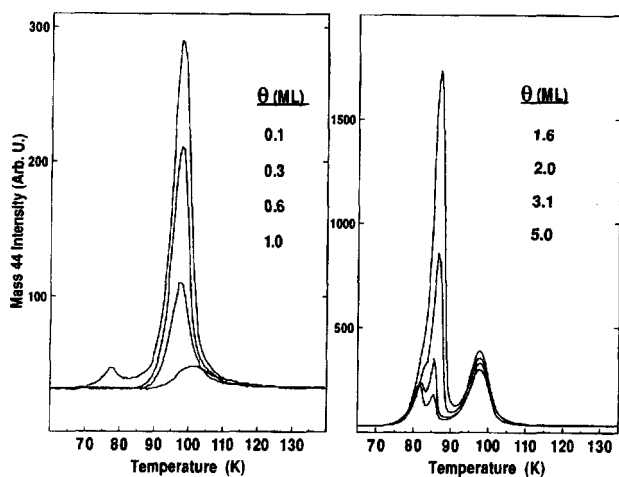


Figure 1. TPD spectra for various N₂O coverages (0.1–5 ML). The dosing temperature was 50 K and the temperature ramp was 4.3 K/s (same in other figures).

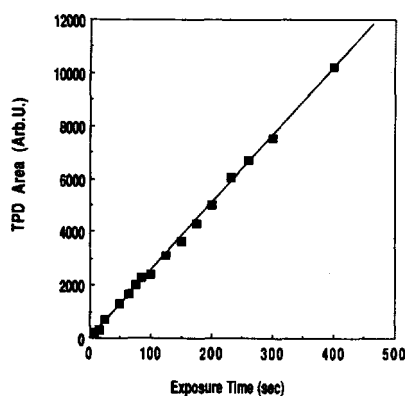


Figure 2. TPD integrated intensities as a function of increasing N₂O exposure.

low-temperature TPD feature was, at first, split into two peaks, but with increased exposure these peaks superimposed, while the peak temperature moved gradually to higher values (86.7 K at 5 ML). This state was not saturable, as expected for a condensed multilayer state.

In Figure 2 the total TPD areas are plotted as a function of dosing time. The linear correlation indicates a constant sticking coefficient regardless of coverage, submonolayer to multilayer.

Care was taken to ensure the 44-amu signal originated from N₂O. The major cracking fragment in the mass spectrometer for N₂O is NO⁺ (30 amu). In TPD, signals of masses 44 and 30 amu were monitored and the ratios checked to ensure that there was no contribution to the measured 44-amu signal from the background CO₂ uptake. It is important to mention that there was no indication of desorption of possible decomposition products (N₂, NO, and O).

Changing the adsorption temperatures of N₂O, below the onset of the monolayer desorption, had no influence on the desorption characteristics (desorption temperature, intensity, and peak shape) of monolayer and submonolayer N₂O. The presence of coadsorbates, however, influenced the desorption of N₂O. Surface oxygen atoms shifted the peak position of monolayer N₂O to higher temperature (by 6 K), while the molecularly adsorbed oxygen caused the opposite effect. Preadsorbed CO inhibited the formation of a monolayer and promoted the appearance of multilayers.²²

3.1.2. XPS Measurements. The XPS spectra for several coverages of N₂O adsorbed at 50 K are shown in Figure 3. Without N₂O adsorption the O(1s) spectrum exhibits a low-intensity peak at around 532.0–533.0 eV due to small amounts of CO and H₂O adsorption from the background. Adsorbed N₂O

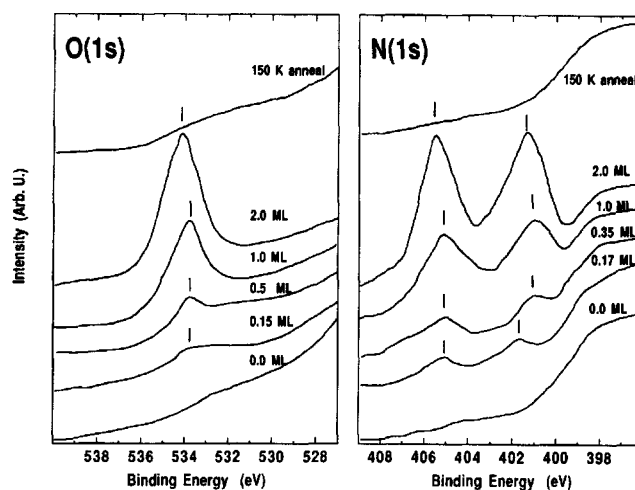


Figure 3. O(1s) and N(1s) XPS of N₂O adsorbed on Pt(111) at 50 K for various coverages (0.15–2 ML). The upper spectra are for a 1 ML dose, warmed to 150 K.

gave only one O(1s) peak centered at 533.9 eV; its intensity increased linearly with the exposure time and, upon reaching the multilayer regime, the peak shifted to higher binding energies. Consistent with the literature,^{13,14,19,21} N(1s) exhibits two peaks, reflecting the different chemical character of the two N atoms in N₂O. At very low coverages, peaks appeared at 401.6 and 405.0 eV. With increasing coverage, the peaks are centered at 401.0 and 405.0 eV, the same energy difference as in the gas phase.²³ We take this shift in binding energy with the coverage as reflecting stronger binding of N₂O (through the N end) at low (submonolayer) coverages, in harmony with our TPD results presented in Figure 1. In the multilayer range the binding energies uniformly shifted to higher values.

Atomic nitrogen (N(1s)) and oxygen (O(1s)) are characterized by binding energies of 397 and 530 eV, respectively, and Figure 3 shows no such features. After heating the surface covered by N₂O to 150 K, the spectrum of a clean surface appeared.

It should be noted that long X-ray exposures (more than 30 min) caused radiation damage of the adsorbed N₂O. This was indicated by the appearance of additional peaks at 402.8 eV for N(1s) and 529.7 eV for O(1s), accompanied by the simultaneously decreased O(1s) and N(1s) intensities for N₂O. Control experiments showed that these new peaks can be attributed to molecularly adsorbed nitrogen and atomic oxygen.²⁴ In order to minimize this X-ray damage, the scan time was restricted to 16 min for each spectrum presented in this paper.

3.1.3. UPS Measurements. For UPS, we used He II (40.8 eV) radiation. Difference spectra for adsorbed N₂O on Pt(111) at 50 K are displayed in Figure 4. Up to 1 ML coverage, four peaks appeared at 5.9, 9.3, 11.0, and 12.8 eV below the Fermi edge. These values are in good agreement with those obtained on Ru(001)^{19,21} and W(110).¹³ The intensity of these features increased with increasing coverage and simultaneously the d-band intensity of Pt continuously decreased. By comparison with the gas-phase spectrum, the levels are assigned as 2 π , 7 σ , 1 π , and 6 σ , in the order of increasing binding energy.²⁵ Above 1 ML of N₂O, all the photoemission peaks uniformly shifted to higher binding energies. At 2 ML they are centered at 6.7, 10.0, 11.8, and 13.6 eV.

Figure 4 also shows the He II spectrum after an N₂O adlayer was warmed to 150 K. No photoemission peaks are observed, consistent with TPD and XPS data showing that N₂O has molecularly desorbed by this temperature. In particular, there is no feature near 6.0 eV that would indicate adsorbed atomic oxygen. These observations and HREELS results¹¹ are in accord with Weinberg's estimate that N₂O thermal decomposition is an impossible process on Pt under these conditions.²⁶

(23) Siegbahn, K. *J. Electron Spectrosc. Relat. Phenom.* 1974, 5, 3.

(24) Kiss, J.; Jo, S. K.; White, J. M. To be published.

(25) Peyerimhoff, S. D.; Bunker, R. J. *J. Chem. Phys.* 1968, 49, 2473.

(26) Weinberg, W. H. *J. Catal.* 1973, 28, 459.

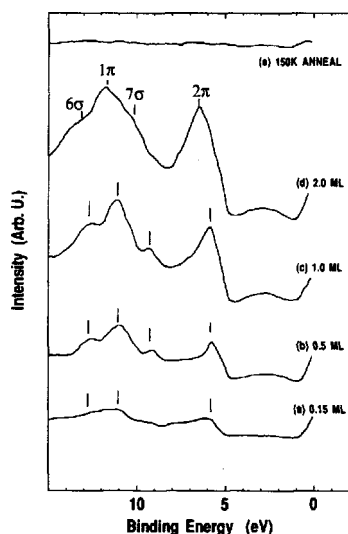


Figure 4. He II UPS (difference spectra) of N_2O adsorbed on Pt(111) at 50 K for various exposures (0.15–2 ML). The uppermost spectrum is for a 2 ML dose warmed to 150 K.

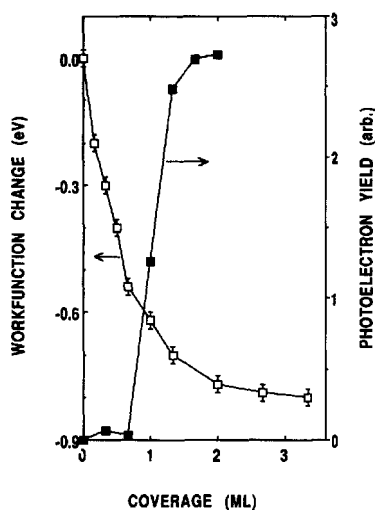


Figure 5. Work function change and photoelectron yield of Pt(111) as a function of N_2O coverage. The photon source for the photoelectron yield measurement was a 100-W Hg arc lamp.

3.1.4. Work Function Measurements. The changes in the work function with N_2O coverage are plotted in Figure 5. The work function decreases continuously with increasing exposure, up to 1 ML coverage, but then approaches saturation at 3 ML ($\Delta\Phi = -0.8$ eV). The work function lowering suggests that there is electron transfer to Pt and that adsorbed N_2O has a positive outward dipole moment. The work function change is not a linear function of coverage even at very low coverages. The curvature indicates that the polarizability of the adsorbed N_2O and/or the depolarization field changes along this curve.

The geometry of the system allows detection of photoelectrons generated during irradiation from the 100-W Hg arc lamp (Figure 5). Clean Pt(111) has a work function of 5.8 eV,²⁷ and the threshold for photoelectron generation is detected, as expected, at about 0.8 ML coverage where $\Delta\Phi \approx -0.5$ eV (the maximum photon energy is 5.3 eV). As compared to the case of $CH_3Cl/Pt(111)$, studied in the same system,²⁸ the yield of photoelectrons here is very small.

3.2. Photochemistry of $N_2O/Pt(111)$. **3.2.1. TDS Results.** Figure 6 shows the TPD spectra of molecular N_2O taken after full-arc (<5.4 eV or >230 nm) irradiations at 50 K for 1 ML initial coverage and various time periods. Two important changes

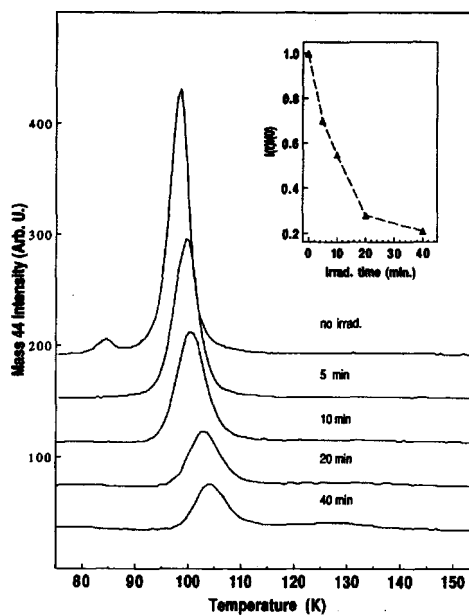


Figure 6. TPD spectra for 1 ML of N_2O adsorbed on Pt(111) as a function of increasing irradiation time. The inset shows the fractional decrease in peak area. The sample was irradiated at 50 K.

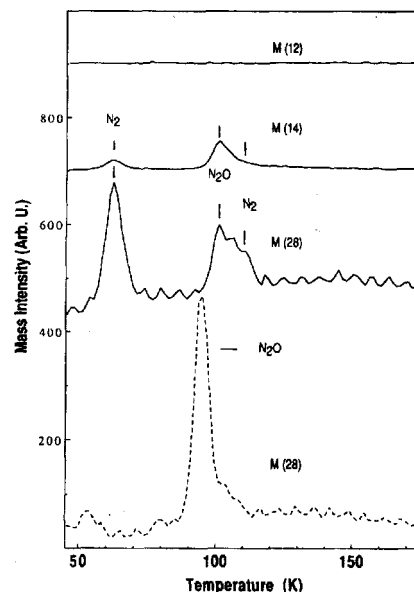


Figure 7. Product distribution after irradiation of 1 ML of N_2O adsorbed on Pt(111) at 50 K. The sample was irradiated for 10 min at 50 K. The dashed curve is the 28 amu cracking fraction in the TPD spectrum of adsorbed N_2O without irradiation.

are obvious. First with increasing irradiation time, a significant amount of N_2O loss was observed. During irradiation, increases were detected in background levels of masses 44, 30, and 28 amu due to cracking patterns of N_2O , indicating N_2O desorption. The other interesting feature of the post-irradiation TPD spectra is that the maximum peak temperature of N_2O desorption increases as a function of irradiation time. This trend was not observed for TPD of N_2O as a function of coverage without irradiation. This result suggests that some surface reaction, leading to products that stabilize the remaining N_2O , also takes place during irradiation.

Figure 7 presents TPD spectra obtained at masses 28, 14, and 12 amu after 10 minutes irradiation of 1 ML N_2O . The dashed curve is mass 28 amu for an unirradiated sample covered by 1 ML N_2O , and kept in the dark for 10 min. The peaks observed at 100 K correspond to N_2O fragmentation in a mass spectrometer. Interestingly, intense new desorption peaks due to molecularly adsorbed N_2 , masses 28 and 14 amu, developed after irradiation at a low temperature. The peak temperature is $T_p = 62.5$ K, and

(27) Kiskinova, M.; Pirug, G.; Bonzel, H. P. *Surf. Sci.* **1983**, *113*, 321.

(28) Jo, S. K.; Zhu, X.-Y.; Lennon, D.; White, J. M. *Surf. Sci.* **1991**, *241*, 231.

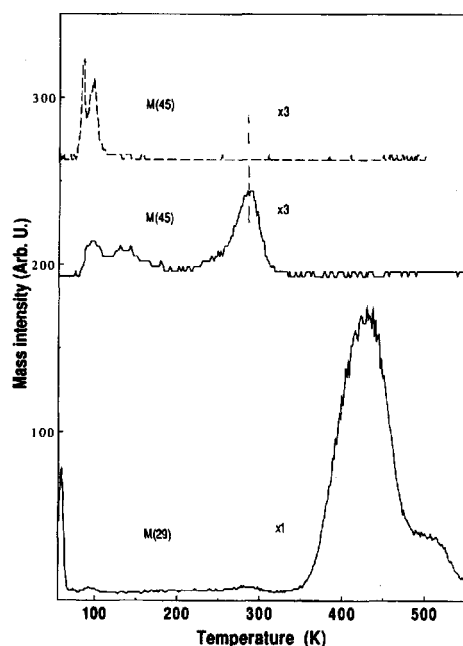


Figure 8. Formation of CO₂ after introduction of CO to irradiated Pt(111) covered by 1 ML of N₂O. The sample was irradiated for 10 min at 50 K. ¹³CO was postdosed at 50 K. The dashed curve represents a spectrum without irradiation. The desorption of unreacted ¹³CO is also shown.

a shoulder appeared around 110 K at these mass numbers. There were no such features at masses 12 and 44 amu, excluding entirely the contributions of CO, CO₂, or N₂O to these new features. The amount of N₂ formed during the photo-induced dissociation increased with the irradiation time up to 20–40 min.

In separate experiments, we also studied the adsorption of molecularly adsorbed N₂ on clean Pt(111) surface at 50 K.²⁴ Most of the physisorbed N₂ desorbed at 60 K, but there was a very small fraction at 113 K. At this point we mention that the recombination of adsorbed atomic N on Pt surfaces occurs at 450–650 K.^{29,30} In this context, we searched for, but found no, recombinative desorption of chemisorbed nitrogen in our photochemistry experiments. We conclude that photon-driven dissociation of N₂O produces little, if any, atomic nitrogen.

Efforts were also made to detect the other dissociation product of N₂O, atomic oxygen, by TPD. As our experimental setup did not allow us to follow the high-temperature desorption of oxygen, we circumvented this problem by titration of atomic oxygen by CO. In order to avoid background contributions, ¹³CO was used. One ML of N₂O was irradiated for 10 min, then 0.5 ML of ¹³CO was postdosed at 50 K. In TPD, the ¹³CO₂ formation was monitored at mass 45 amu. Figure 8 shows a significant amount of ¹³CO₂ desorption with T_p = 288.5 K. This peak temperature agrees quite well with published data obtained in the reaction of CO ad molecules with oxygen adatoms on a Pt(111) surface.³¹ This desorption peak could not be observed when the adsorbed N₂O was not irradiated before CO dosing (uppermost curve in Figure 8).

The time-dependent loss of the parent molecule during irradiation, as determined by TPD, can be used as a quantitative measure of the photon-driven rate. Semilogarithmic plots of the fractional decrease in the TPD signal as a function of irradiation time for a range of initial coverages were all linear. From the slopes, we can determine the effective cross section, σ , as a function of coverage. Since only photon energies exceeding 4.35 eV are effective, we can use the power flux (85 mW/cm²) transmitted,

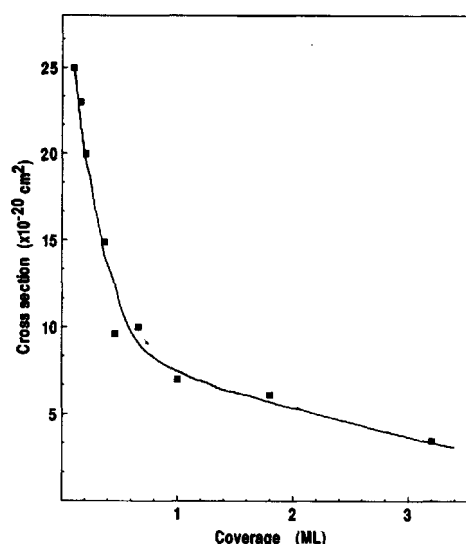


Figure 9. Effective cross section for the photon-driven total loss, (i.e., desorption and dissociation) of N₂O on Pt(111) at 50 K.

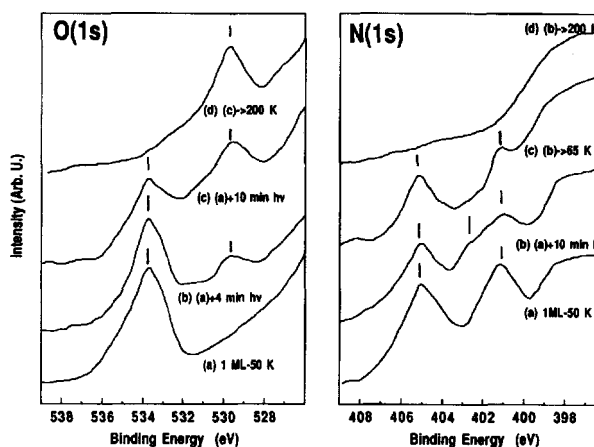


Figure 10. O(1s) and N(1s) XPS of 1 ML of N₂O on Pt(111) at 50 K as a function of irradiation time. The changes due to warming after irradiation are also indicated.

with a 285-nm cutoff filter in place, to calculate the cross section. By subtraction from the full-arc flux (100 mW/cm²), we calculate that the 285-nm cutoff filter limits the active power flux at the sample to 15 mW/cm². In the distribution of UV photons from as Hg arc,³² a broad peak at 254 nm is the main contribution between 285 nm and the intensity onset wavelength of 230 nm. Therefore, it is reasonable to represent the average power between 230 and 290 nm with 254 nm photons. Thus, the effective photon flux, n , is 1.9×10^{16} photons/(cm² s). σ is given by k/n , where k is the first-order rate constant obtained from the semilogarithmic plots. The resulting cross section decreases with increasing coverage (Figure 9) and the decrease is more pronounced at low coverages.

3.2.2. XPS Measurements. The effects of UV irradiation upon XPS spectra of 1 ML of N₂O are shown in Figure 10. The intensity of the O(1s) peak (533.9 eV) for adsorbed N₂O decreased with the irradiation time and a new photoemission peak developed at 529.7 eV, which was not detected in the dark. This species is assigned as adsorbed atomic oxygen formed by photodissociation of adsorbed N₂O. The intensity of this feature remained unchanged when the sample was warmed to 200 K. The irradiation also reduced the intensities of the two N(1s) peaks at 401.0 and 405.0 eV and a new feature appeared near 402.8 eV. This new photoemission disappeared when the surface was heated to 65 K, below the onset of N₂O desorption. TPD results showed that N₂ desorption occurs in this temperature range. On the other hand,

(29) Schwaha, K.; Bechtold, E. *Surf. Sci.* **1977**, *66*, 383.

(30) Kiss, J.; Berko, A.; Solymosi, F. In *Proceedings of the 8th International Vacuum Congress and 4th International Conference on Solid Surfaces*; Degraas, D. A., Costa, M., Eds.; Societe Francaise du Vide: Cannes, France, 1980; p 521.

(31) Matsushima, T. *Surf. Sci.* **1983**, *127*, 403.

(32) White, J. M. Ph. D. dissertation, University of Illinois, 1966.

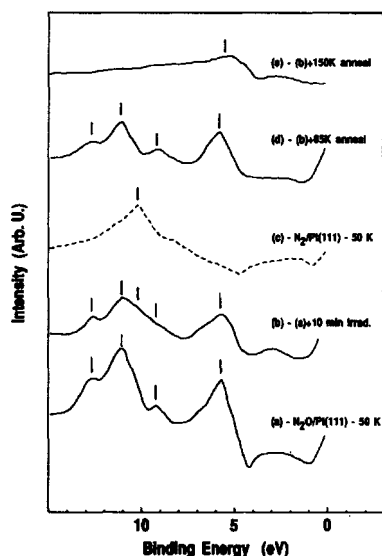


Figure 11. Effects of irradiation on He II UPS (difference spectra) of 1 ML of N_2O on Pt(111) at 50 K. Irradiation time was 10 min. The effects of warming after irradiation are also shown. For comparison, the dashed curve shows the UPS spectrum of molecularly adsorbed nitrogen on Pt(111) at 50 K.

we have found that adsorbed N_2 exhibits the same binding energy peak (402.8 eV) on a Pt(111) surface.²⁴ Thus, we attribute this feature to molecularly adsorbed nitrogen formed during N_2O photodissociation. Atomic nitrogen is characterized in XPS by a binding energy of approximately 397 eV on metal surfaces.¹³ Since no such features are observed in Figure 10, we suggest that N–N bond breaking does not occur during irradiation.

From a comparison of areas of O(1s) peaks, before and after irradiation, we estimate that 10-min irradiation results in 70% desorption and 30% dissociation at 1 ML initial coverage of N_2O . With decreasing initial coverage, the dissociation pathway increases, compared with the desorption. At 0.5 ML, 50% dissociates, while at 0.2 ML, this value is about 80%.

3.2.3. UPS Measurements. The effect of irradiation upon the He II UPS spectrum of 1 ML of N_2O is shown in Figure 11. After 10-min irradiation a reduction in intensity of the N_2O peaks could be observed. In addition to this, the shape of 1π emission, centered at 11.0 eV, has modified by a low-energy tailing, indicating that a new peak has appeared, somewhere around 10.0 eV. This feature disappeared when the sample was heated to 65 K, where the N_2 desorption is completed. Separate control experiments showed that the physisorbed N_2 on Pt(111) has a strong photoemission at this binding energy (dashed line in Figure 11).²⁴ It is difficult to confirm a contribution from dissociated oxygen in Figure 11; adsorbed oxygen atoms produce a broad peak at 6.0 eV, and this binding energy coincides with the N_2O 2π state, which remains intense after 10-min irradiation. When the adlayer is warmed to 150 K, desorbing the N_2O , the remaining feature at 5.5 eV can be attributed to adsorbed oxygen, an observation suggesting the partial photodissociation of N_2O molecules.

3.2.4. Wavelength Dependence. Cutoff filters were used to determine that wavelengths were causing the observed photoeffect. Various N_2O coverages were irradiated for 20 min by using a 285-nm cutoff filter, and within experimental error, no reduction in TPD area was found. Thus, only wavelengths below 285 nm (>4.35 eV) play a role in the observed photochemistry. Additionally, regardless of the N_2O coverage, no photoelectrons were detected when the 285-nm cutoff filter was used.

4. Discussion

Consider first the thermal properties of the $\text{N}_2\text{O}/\text{Pt}(111)$ system. As a function of dosing time, the total TPD areas grow linearly from submonolayer through multilayers. The low TPD peak temperatures (monolayer and multilayer) underscore the very weak bonding of N_2O to Pt(111) and a small difference between the monolayer and multilayer desorption energies.

In the submonolayer coverage regime (below 0.3 ML), there is some evidence, based on the N(1s) XPS spectra and TPD, that N_2O is bound more strongly than at higher coverages. At low coverages the desorption appears at higher temperatures, in agreement with the fact that the terminal nitrogen XPS exhibits a higher binding energy. From the work function experiments we may also conclude that N_2O binds via the terminal nitrogen atom in harmony with HREELS results obtained on this surface¹¹ and Ru(001).²⁰ We presume that N_2O acts as a soft Lewis base, forming a donor bond, presumably with 7σ nonbonding orbital (located on the terminal nitrogen) with little back donation into the unoccupied antibonding 3π orbital. The back donation is unproven, but if it occurs this orbital will not be highly localized. We cannot exclude that the higher binding energy state belongs to some defect sites of Pt, although different sputtering times or annealing temperatures did not influence this feature. We have to mention that a continuous shift of the TPD peak temperature with increasing coverage was observed on Ir(III) in the submonolayer range.¹² In the case of Pt(111), the peak temperatures do not change above 0.3 ML.

Above 0.3 ML all XPS and UPS peaks above the same energy separation as in the gas phase. Above 1 ML coverage the binding energies shifted uniformly to higher values, indicating that the proper reference level is the vacuum level. The HREELS results¹¹ demonstrated that, up to monolayer coverage, the N_2O was tilted at approximately 35° to the plane of the surface. For multilayer coverages, the N_2O was believed to be nearly parallel to the surface. All these data strongly suggest that N_2O is weakly chemisorbed in the monolayer regime. These observations may help to understand the nature of the photochemistry of N_2O on a Pt(111) surface. The TPD, XPS, and UPS data show that a clean surface is restored by heating any coverage of N_2O to 150 K. Clearly, there is no thermal dissociation in this system, making photon-driven processes easy to identify.

Turning to photoeffects, we note that photon-driven dissociation is evident from the desorption of N_2 , a shift to higher temperature (stabilization by atomic oxygen) of residual N_2O , and the growth, with irradiation time, of O(1s) and N(1s) peaks characteristic of atomic oxygen and adsorbed molecular nitrogen, respectively. Photon-driven desorption is evident in the loss of XPS intensity, N(1s), and O(1s), UPS bond intensity, and TPD area of N_2O . Dissociation is more significant at low coverages; desorption becomes dominant above half a monolayer (70% at 1 ML).

The wavelength response is very interesting. At the coverages studied (0.5 and 1.33 ML), there was no photochemistry with the 285-nm cutoff (<4.35 eV) filter. This means that lowering the work function by 0.62 eV (5.8–5.18 eV) does not promote either desorption or dissociation. In this regard, it is clearly not simply a matter of producing photoelectron energies above vacuum level. As shown by comparing Figures 5 and 9, an increase in the photoelectron yield in the 0.7 to 2 ML regime is accompanied by a steady drop in the reaction cross section. Moreover, the reaction cross section is highest when there are no photoelectrons. In contrast, photoelectrons do play an important role in the photo-dissociation of CH_3Cl on Pt(111).²⁸

We favor substrate excitation followed by electron attachment as a mechanism for both dissociation and desorption, for the following reasons: (1) gas-phase N_2O is nearly transparent unless photons have wavelengths below 210 nm⁶ (e.g., the cross section at 240 nm is less than 10^{-23} cm²); (2) the interaction with Pt(111) is very weak; (3) it is well-known that gas-phase N_2O captures an electron;^{33,34} and (4) adsorbed N_2O ($\text{N}_2\text{O}/\text{Ru}(001)$) is easily dissociated by an electron beam to give $\text{N}_2(\text{g})$, $\text{NO}(\text{g})$, and $\text{O}(\text{a})$.²¹ While we do not rule out some contribution from direct adsorbate–substrate excitation, it noteworthy that direct evidence for this kind of process within the first monolayer is rare,^{35,36} and most

(33) Schulz, G. J. *J. Chem. Phys.* **1961**, *34*, 1778.

(34) Yamamoto, S.; Mitsuke, K.; Misaizu, F.; Kondow, T.; Kchitsu, K. *J. Phys. Chem.* **1990**, *94*, 8250.

(35) Zhu, X.-Y.; Hatch, S. R.; Campion, A.; White, J. M. *J. Chem. Phys.* **1989**, *92*, 5011.

(36) Zhou, X.-L.; White, J. M. *J. Chem. Phys.* **1990**, *92*, 1504.

evidence favors substrate excitation. In any case, it is clear that a single monolayer of the adsorbate-substrate complex adsorbs, at most, very little light and that by far the largest fraction of the absorption occurs in the Pt.

Consider an electron attachment model. In the gas phase, the electron affinity of N₂O is +0.24 eV.⁸ In a molecular orbital description, this electron populates the lowest unoccupied molecular orbital (LUMO) of N₂O, 3p, forming N₂O⁻, which is 0.24 eV more stable than a separated (N₂O, e) pair and which is thermodynamically unstable with respect to N₂ and O⁻ (entropy is important here). Potential energy curves have been presented that, because of the observation of stable N₂O⁻ ions, have a small minimum (= 0.5 eV) with respect to dissociation into N₂ and O⁻.⁹ The attachment cross section has a resonance peaking at 2.2 eV (= 1 eV fwhm), which is strongly temperature dependent (any vibrational excitation dramatically increases the cross section).

Turning to adsorbed N₂O, we have UPS and XPS data indicating, as expected, that the orbitals are pinned to the Fermi level of the system since the peak positions (Figures 3 and 4) remain constant as the work function changes. Thus, taking 5.8 eV as the reference work function for the first monolayer of N₂O, the binding energy (BE) of the 2π orbital is 11.5 eV (5.9 + 5.8 eV), compared to 12.9 eV in the gas phase. The 1.4 eV difference is attributable to the combined effects of initial- and final-state interactions with the metal. The initial-state shifts arise, even in the absence of chemical interactions, because the adsorbate lies within the surface dipole field. The effect is to move all the molecular orbitals further below the vacuum level. If there were no final-state relaxation by the metal, the orbital BE's would all increase when measured with respect to the vacuum level. This same argument holds for the LUMO, and we expect that, compared to gas-phase situations, the electron attachment resonance will be broadened (>1 eV fwhm) and, at least in part, move below the vacuum level. A resonance centered beneath the vacuum level would account for both the high cross section for subvacuum-level electrons and the lack of sensitivity to low-energy photoelectrons. Assuming a constant distribution of incident photons and taken the LUMO as pinned to the Fermi level, then the latter moves upward as the work function decreases but its position remains fixed with respect to the distribution of excited electrons. To be effective, excited electrons, formed in the bulk, must migrate to the surface where we assume they encounter and must pass a barrier that lies in the interface between the metal and the adsorbed N₂O. As the work function decreases, this barrier also decreases and we expect a larger number of electrons to be able to pass to the adsorbate, assuming the photon energy exceeds the threshold or comes close enough to make tunneling significant.

The work function at 1.33 ML is 5.20 eV; thus, with the 285-nm cutoff filter in place, the available photons bring excited electrons to within 0.85 eV of the vacuum level. But there is no photon-driven chemistry. At the lowest coverage studied with the full arc (5.3-eV photons and Φ = 5.6 eV), excited electrons are brought to within 0.3 eV of the vacuum level and the cross section reaches its highest value. Reducing the work function to 5.3 eV, by increasing the coverage, brings excited electrons to the vacuum level, but the cross section drops. Pieced together, these results can be modeled by assuming a strong attachment resonance lying between 0.3 and 0.85 eV below the vacuum level. For the first monolayer, then, the number of excited electrons produced in this range would control the cross section.

The negatively charged N₂O, following in the footsteps of the highly successful Antoniewicz model,³⁷ will be attracted toward the surface by image forces and, simultaneously, will be adjusting

its internal geometry to reach the equilibrium configuration. These configuration changes may involve lengthening the N-O bond and decreasing the N-N-O angle. Quenching to the ground electronic state, in regions where the total energy is greater than the adsorbed N₂O binding energy, can lead to desorption as a neutral, since part of its vibrational energy might transfer to the N₂O-Pt bond. A very similar explanation was applied to the photo-induced desorption of NO on Pt(111)³⁸ and Ag(111)³⁹ and of SO₂ on Ag(111).⁴⁰

Dissociation is another relaxation pathway. The electronically quenched species can be excited in the N-O stretch; this could be sufficient for dissociation into O(a) and N₂(a). The standard enthalpy of formation of N₂O is 19.49 kcal/mol and of O(g) is 59.159 kcal/mol. Thus, the gas-phase dissociation of N₂O into N₂ and O is 39.67 kcal/mol endothermic. Since the binding energies of N₂ and N₂O to Pt(111) are roughly the same (there is only 30-40 K difference in desorption temperatures), the stability of the system is governed by the O-Pt bond strength. Thus, thermodynamics strongly favors the formation of N₂ and O(a).

As we discussed above, there is some TPD and XPS evidence that N₂O bonds more strongly to Pt(111) at low, compared to high, coverages. The work function change deviates from linearity with increasing coverage, which means that the local potential (effective dipole moment) decreases. The stronger interaction probably leads to a slightly shorter adsorbate-substrate distance. Formation of weaker bonds, with increased coverage, will lengthen the adsorbate-substrate distance, raise the local potential barrier that the hot electron must cross, and lower the excitation cross section.

Empirically, the ratio of the photo-induced dissociation to the desorption decreases with increased initial coverage of N₂O. One simple mechanistic approach that will account for this is the following: oxygen freshly formed during dissociation may displace neighboring adsorbed N₂O, leading to desorption of the latter even at the irradiation temperature. In other words, the reactive O atoms force out adsorbed N₂O. This process may contribute to the photodesorption yield. While we cannot entirely exclude this possibility, a more likely explanation for the change of dominant reaction pathways is that, with increasing initial coverage, N₂O blocks the dissociation step as it requires bare neighboring substrate atoms. This inhibition process can also contribute to the decay for the average cross section in the submonolayer regime.

5. Summary

The work reported here can be summarized as follows: (1) Nitrous oxide, N₂O, adsorbs molecularly on Pt(111) at 50 K. (2) Desorption occurs, without decomposition, in two peaks, a multilayer peak at 85 K and a monolayer peak at 97 K. (3) Irradiation of adsorbed N₂O with photons having energies exceeding 4.35 eV leads to both dissociation and desorption. (4) The total cross section for loss of N₂O lies between 10⁻¹⁹ and 10⁻²⁰ cm². (5) Since nitrous oxide is very weakly and molecularly held and since it is transparent for the photon energies used here, we attribute the observed photon-driven chemistry to the action of electrons excited above the Fermi level but below the vacuum level of the substrate.

Acknowledgment. Financial support by the National Science Foundation (CHE 9015600) is gratefully acknowledged.

Registry No. N₂O, 10024-97-2; Pt, 7440-06-4; N₂, 7727-37-9; O, 17778-80-2; ¹³CO, 1641-69-6; ¹³CO₂, 1111-72-4.

(38) Buntin, S. A.; Richter, L. J.; Cavanagh, R. R.; King, D. S. *Phys. Rev. Lett.* **1988**, *61*, 1321.

(39) Franchy, R.; So, S. K.; Ho, W. *Vacuum* **1990**, *41*, 284.

(40) Castro, M. E.; White, J. M. To be published.

(37) Antoniewicz, P. R. *Phys. Rev. B*, **1980**, *21*, 3811.